Featured in Physics

Hydrodynamic Mechanism for Clumping along the Equatorial Rings of SN1987A and Other Stars

Michael J. Wadas,[*] William J. White, Heath J. LeFevre, Carolyn C. Kuranz, Aaron Towne, and Eric Johnsen

University of Michigan, Ann Arbor, Michigan 48109, USA

An explanation for the origin and number of clumps along the equatorial ring of Supernova 1987A has eluded decades of research. Our linear analysis and hydrodynamic simulations of the expanding ring prior to the supernova reveal that it is subject to the Crow instability between vortex cores. The dominant wave number is remarkably consistent with the number of clumps, suggesting that the Crow instability stimulates clump formation. Although the present analysis focuses on linear fluid flow, future nonlinear analysis and the incorporation of additional stellar physics may further elucidate the remnant structure and the evolution of the progenitor and other stars.

The recency and proximity of Supernova 1987A (SN1987A) to Earth make it an unparalleled source of astrophysical data shaping our understanding of stellar evolution [1–3]. Light from the supernova initially illuminated a complex three-ring structure surrounding the progenitor consisting of an approximately circular equatorial ring (ER) [4], with the progenitor at its center, and two outer rings roughly coplanar and axisymmetric with the ER, but with larger radii and offset in the polar directions. Telescopic observation indicates that the ER consists of between 30 and 40 clumps of mass nearly evenly spaced along the ring [5,6]. Approximately 5600 d after the collapse of the progenitor, the blast wave from the supernova reached the ER, heating and illuminating the clumps, commonly referred to as "hot spots," shown in Fig. 1(a) [5,7–11].

Several theories describe the origin of the ER. The expansion velocity and radius, $V_{ER} = 10.3$ km s^{-1} [13] and 0.6 ly [14], respectively, of the ER before the blast suggest it was formed from mass ejected by the progenitor 20 000 yr prior to the supernova [3]. Leading theories explain the mass ejection as the result of a binary star merger [15–17] and/or the interaction of stellar winds from different stages of the progenitor evolution [18–20], while additional theories evoke magnetic fields [21], polar jets [22], or a pre-existing protostellar disk [23].

Despite the extensive effort to understand the rings, little is known about the origin of the clumps comprising the ER, which are imbedded in the innermost region of a surrounding interclump annulus [24–28] that the leading shock from the supernova has recently exited [29–32]. Past studies assert that the clumping is the result of hydrodynamic forces [4,33], but do not identify the specific mechanism or explain the observed number of clumps. Other work suggests that the clumps are spikes due to the Rayleigh-Taylor fluid instability [34,35] but requires un-evidenced mechanisms and is still unable to predict the number of clumps [22,36,37].

We propose that the formation of the clumps is indeed driven by hydrodynamics but results from the Crow instability (CI) between vortex cores. Our analysis considers the stability of perturbations along an annular torus ejected from the progenitor, a common feature of theories describing the three-ring nebula, and yields a dominant unstable wave number consistent with the number of observed clumps. In this Letter, we first describe the CI and how it relates to the expanding ER. Next, we present the stability analysis. We conclude with a discussion of the relevance of our stability analysis to other star systems exhibiting ERs.

The CI describes the growth of perturbations along interacting vortex cores [38–40]. Originally studied in planar geometries relevant to aircraft wing-tip vortices [41], the CI was later observed along radially expanding vortex dipoles [12,42–45]. Perturbations along the interacting cores grow until they touch, triggering a complex reconnection process resulting in the pinch-off of isolated vortex structures, as shown in Fig. 1(b) [12,46–49].
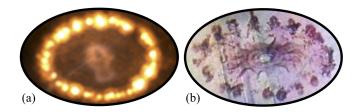

FIG. 1. Hot spots along the equatorial ring of SN1987A [5,11] (a) and pinch-off of isolated vortex structures from a radially expanding vortex dipole in water [12] (b). Images are reproduced with permission.

The expanding ER in SN1987A likely acquired vorticity from its interaction with stellar wind from the progenitor [18–20]. This vorticity, equal and opposite in magnitude on opposing sides of the equatorial plane given the symmetry of the ER, would cause the ER to develop into an expanding vortex dipole [20,50] potentially unstable to the CI. The subsequent growth of perturbations would then result in pinch-off into the observed isolated clumps.

Our analysis therefore considers the stability of two circular vortex cores of opposite circulation, an integrated measure of vorticity, forming a radially expanding vortex dipole. Figure 2 shows a schematic of the setup involving two vortex cores with circular cross sections of thickness c, separation distance b, radius R, and circulation magnitude Γ, with core-displacement perturbations in the azimuthal direction θ, of integer azimuthal wave number k. While the expanding torus leading to the formation of the vortex cores is a common feature among theories describing the ER of SN1987A, we evoke the binary-merger theory of Refs. [16,17] to initialize our stability problem. According to this theory, as the radius of the binary orbit between a red supergiant and a companion decreased, mass transfer between the two stars formed a common envelope that, due to its angular momentum, was elongated in the equatorial plane forming a torus of radius $R_T = 3 \times 10^{12}$ m and thickness $D_T = 2 \times 10^{12}$ m. After the stars merged, wind from the newly formed blue supergiant (BSG) began to blow over the torus at approximately $V_{\mathrm{BSG}} = 550$ km s^{-1} [51], forming the vortex dipole and initializing its radial expansion.

We therefore estimate the circulation available for the formation of the vortex cores to be $\Gamma = V_{\mathrm{BSG}} D_T$ [52,53]. Following Refs. [51,54], we consider a blue supergiant wind environment formed from a constant stellar mass ejection rate of $\dot{m}_{\mathrm{BSG}} = 1 \times 10^{-6} M_\odot$ yr^{-1}, pressure $p_{\mathrm{BSG}} = 1 \times 10^{-6}$ Pa, and temperature $T_{\mathrm{BSG}} = 1.5 \times 10^4$ K [4].

Following potential theory, the velocity at the center of each core is governed by the Biot-Savart law,

$$U_n = \sum_{m=1}^{2} \frac{\Gamma_m}{4\pi} \int \frac{L_{mn} \times dS_m}{|L_{mn}|^3}, \qquad (1)$$

where $n = 1$ or 2 denotes the top or bottom core, respectively, L_{mn} is the displacement vector to a point on core m from a point on core n, and dS_n is the differential tangent vector. Equation (1) holds provided that the flow is incompressible, inviscid, and continuous, which is supported by the Mach, Reynolds, and Knudsen numbers, respectively, relevant to the expanding ring. For an ideal gas, the Mach number is

$$M = \frac{V_{\mathrm{BSG}} - V_{\mathrm{ER}}}{a} = (V_{\mathrm{BSG}} - V_{\mathrm{ER}})\sqrt{\frac{\rho}{\gamma p}}, \qquad (2)$$

where a is the sound speed, $\rho = \dot{m}_{\mathrm{BSG}}/4\pi R^2 V_{\mathrm{BSG}}$ is the density, and $\gamma = 5/3$ is the adiabatic index. The Reynolds number is

$$\mathrm{Re} = \frac{\Gamma}{\nu} = \frac{\Gamma}{2.3 \times 10^{-16}\sqrt{A}T_{\mathrm{BSG}}^{5/2}/\Lambda Z^4 \rho}, \qquad (3)$$

where ν is the kinematic viscosity [55,56], A is the atomic mass of the gas (assumed to be hydrogen for simplicity) in atomic mass units, $\Lambda = 10$ is the Coulomb logarithm, and Z is the atomic number of the gas, with all dimensional quantities expressed in Systeme International units. Finally, the Knudsen number is related to the Mach and Reynolds numbers,

$$\mathrm{Kn} = \frac{\lambda}{D_T} = \frac{M}{\mathrm{Re}}\sqrt{\frac{\gamma\pi}{2}}, \qquad (4)$$

where λ is the mean free path.

Figure 3 shows the radial dependence of the Mach, Reynolds, and Knudsen numbers according to Eqs. (2)–(4). Shortly ($\sim$400 yr) after the binary merger, the flow enters a regime where $M \lesssim 0.3$, Re $\lesssim 10^3$, and Kn $\lesssim 10^{-3}$, which endures for approximately 18 000 yr, as indicated by the shaded region in Fig. 3. During this time, the incompressible, inviscid, and continuous assumptions are
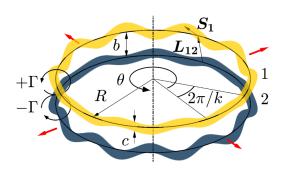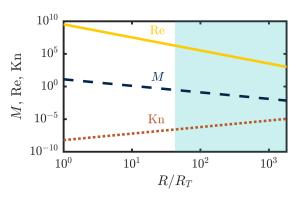

FIG. 2.   Schematic of the stability analysis parameters. Red arrows indicate the direction of the dipole expansion.

FIG. 3.   Mach (blue dashed), Reynolds (yellow solid), and Knudsen (orange dotted) numbers versus radius. The teal shaded region satisfies $M < 0.3$, Re $> 10^3$, and Kn $< 10^{-3}$.

well supported, such that the expanding torus would be subject to the formation of vortex cores unstable to the CI.

Recent work [57] examines the cylindrical CI governed by the Biot-Savart law for the setup in Fig. 2, which we apply presently. Equation (1) is linearized, a normal-mode ansatz is assumed for perturbations, and first-order coefficients are organized into a matrix-eigenvalue problem. The solution yields growth rates, α_k, where the subscript denotes the wave number, for a symmetric mode where perturbations on one core grow as a mirror image of those on the other. Because the zero-order motion (i.e., the core radius, core separation distance, and core thickness) is not constant, the growth rate is a function of time and therefore integrated to determine the perturbation spectrum. The effect of viscosity on the zero-order motion is considered in Ref. [57] but presently neglected due to the initially large Reynolds number. Instead, the radial vorticity distribution within each core is assumed Gaussian such that the boundary of the core is located at 2 standard deviations from the maximum vorticity at the core center, consistent with experimental measurements of vortex boundaries and vorticity distributions [43,44,58–60]. We refer readers to Ref. [57] for additional detail.

We initialize the stability analysis 400 yr after the binary-merger event, when the flow is approximately incompressible, inviscid, and continuous. By this time, the torus would have expanded to a radius $R_0 = R_T + V_{ER} \times 400$ yr. Based on past studies examining vortex dipole formation from laterally accelerated cylinders [59,61,62], we estimate the torus would form a vortex dipole with initial core separation distance and thickness $b_0 = D_T/2$ and $c_0 = b_0/2$, respectively. Perturbation amplitudes h_k, where the subscript denotes the wave number, are initialized as a uniform spectrum equal to the smallest continuum length scale, i.e., $h_k(t=0) = \lambda/Kn_{max}$, where $Kn_{max} = 10^{-3}$.

Figure 4 presents the results of the stability analysis applied to SN1987A in terms of the growth rate and the perturbation amplitude of the symmetric mode as a function of wave number and time, with quantities nondimensionalized by the initial radius and circulation magnitude. While the range of excited wave numbers is always bounded by $k = 1$, the outward expansion of the dipole tends to stimulate perturbation growth at higher wave numbers, widening the range of wave numbers experiencing growth. However, due to the sign of the circulation in each vortex, the cores separate (i.e., b increases) as they expand outward, which tends to narrow the range of wave numbers experiencing perturbation growth and decrease the growth rate. The influence of the outward expansion on the wave number range is greater, and the net result of this competition is therefore a widening range of wave numbers supporting perturbation growth, but with decreasing growth rates, as Fig. 4(a) shows.

Symmetric perturbations grow until their amplitude is on the order of the core separation distance, which first occurs
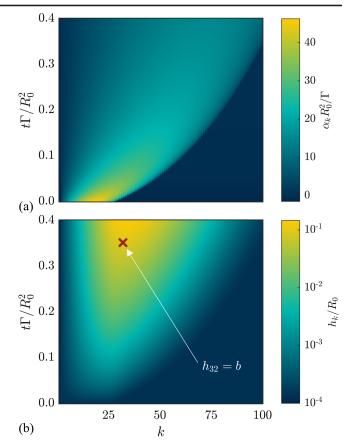

FIG. 4. The growth rate (a) and perturbation amplitude (b) of the symmetric mode versus wave number and time. The red X denotes the time and wave number when the maximum perturbation equals the core separation distance.

for a wave number of $k = 32$ at the time indicated by the red X in Fig. 4, corresponding to a dimensional time of 160 yr, or 560 yr following the binary merger. The dominant wave number of the CI, which corresponds to the number of pinched-off secondary vortex structures (see Fig. 1), is remarkably close to the observed number of hot spots in SN1987A. In addition, other wave numbers experiencing significant perturbation growth would introduce variability in the pinch-off locations, yielding secondary vortex structures with different sizes, which accounts for the range of observed hot spot sizes in the ER of SN1987A, including additional smaller clumps that may escape detection given current measurement resolution. Furthermore, the dynamics associated with perturbation growth occur well within the time frame during which the governing equations, derived from the Biot-Savart law, are valid.

The dominant wave number is largely insensitive to the geometry of the initial torus and subsequent dipole except for a decrease in the ratio between the separation distance and radius, b_0/R_0. Generally, this insensitivity supports the claim that the CI is responsible for clumping in S1987A (i.e., tuning these parameters is not required to match the

dominant wave number and number of clumps). Moreover, given that we use the geometry implied by Refs. [16,17] to initialize our stability problem, the sensitivity to b_0/R_0 combined with the agreement between our theory and observations supports the hypothesis described therein, though other models, including other interacting wind theories [18–20], can produce similar structures. Although in the model of Refs. [16,17] the source of vorticity is wind from the blue supergiant shearing past the remnant of the envelope established during the binary phase of the progenitor, the clumps are immersed in gas interpreted as the remnant of the red-supergiant wind [25–27]. If, instead, the red-supergiant wind (e.g., the wind described in Ref. [51]) drives the flow, perturbation growth commences earlier, i.e., with greater b_0/R_0, compared to the scenario where the dynamics are driven by the blue-supergiant wind. However, due to the relative insensitivity of the dominant wave number for large b_0/R_0, the dominant wave number decreases by only 7 and is therefore still roughly consistent with observations.

To illustrate the dynamics predicted by our stability analysis, Fig. 5 shows a simulation performed using our in-house, finite-volume hydrodynamics code solving the two-fluid Euler equations [63]. The ER is initialized as a torus geometrically scaled to the ER 400 yr following the binary merger and immersed within a radial outflow with $M = 0.3$, simulating the stellar wind. The torus cross section has constant radial axis thickness τ and perturbed vertical axis thickness, $\tau[1 + 0.1\sin(2\pi\theta \times 32)]$. Because computational constraints limit the resolvable amplitudes, the perturbation can only be simulated through a small portion of its growth from an initial amplitude, on the order of the smallest continuum length scale, to the core separation distance. Still, the simulation demonstrates the key physics. The torus rolls up into an expanding vortex dipole, identified by an isosurface of the Q criterion [64], which indicates the intensity of rotational relative to straining motions. An isosurface of the mass fraction,

which identifies fluid comprising the initial torus, is also shown.

As the dipole forms, a thin annulus of the original torus fluid is shed into the wake of the vortex cores, which is seen in experiments of dipole formation [12,61,62]. This feature is consistent with the well-documented thin annulus comprising the interclump portion of the ER, which starts at the radial location of the clumps and extends to larger radii [28,65–68]. The simulation shown in Fig. 5 indicates that the mass comprising the original torus is split nearly evenly between the clumps and the annulus, consistent with modern-day observations [4,68,69]. This agreement suggests that the initial cross-sectional aspect ratio of the ER was of order unity, which is well supported by research on the formation of vortex cores [52,53,70], whereas a relatively more massive and extended interclump region would be expected for initially thinner ERs. Furthermore, diffusion and gravity support the observed enhanced density of the clumps compared to the annulus [68]. Assuming that the clumps and annulus initially have the same diffusion coefficient and interface-normal density profile, the initial rate at which the density of the annulus decreases compared to the clumps is proportional to the surface area ratio between the annulus and clumps, which we calculate to be approximately 12 in our simulation, though it would increase as the annulus continues to stretch to larger radii. Given that mass in a clump is, on average, nearer to the center of mass of the clump compared to the proximity of mass in the annulus to the annulus cross-sectional center of mass, gravity would further compound the relative density enhancement of the clumps.

The CI causes the vortex core perturbations to grow to the point where nonlinear effects initiate the vortex reconnection process, leading to the pinch-off of 32 isolated vortex structures, i.e., clumps. The complete pinch-off of these structures is not required for the formation of clumps in astrophysical systems. Once the CI sets the number of locations where the ER starts to thin, corresponding to the dominant wave number, other physics, including gravitational and radiative effects, may become relevant to completing the clump formation [71]. Furthermore, additional hydrodynamic mechanisms, including the Rayleigh-Taylor instability, may explain the emergence of fainter clumps recently observed at higher latitudes [4,10,32,72]. Finally, because vorticity is advected into the wake of the dipole along with fluid comprising the original torus, additional vortices may form at larger radii, stimulating the formation of a ring of smaller clumps consistent with recent observations [6].

While the focus of the present work is the ER of SN1987A, the CI could govern clumpy circumstellar gas surrounding other stars, including Fomalhaut [73], WeBo 1 [74], SBW1 [75], HR 4796A [76], HD 98800 [77], and many others [78]. While these systems do not all exhibit the three-ring structure of SN1987A, similar
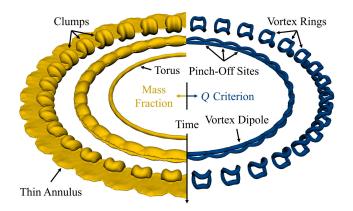

FIG. 5. Isosurfaces of mass fraction (left) and Q criterion (right) at times $t\Gamma/R_0^2 \in (0, 0.1, 0.7)$, which increase with increasing radius.

hypotheses (e.g., binary merger, transition from a red to a blue supergiant, etc.) explain the formation of many observed ERs, which would similarly be subject to clump formation via the CI. Moreover, many of these ERs are thought to be protoplanetary disks, suggesting the clumping mechanism described in the present work may be a precursor to the formation of orbital bodies in these and other systems, possibly including our own solar system.

In this Letter, we propose that clumping in the ER of SN1987A and other star systems may be caused by the CI. Our stability analysis shows the dominant unstable wave number is consistent with the number of observed hot spots, suggesting that the CI initiates and sets the number of clumps. In other systems that do not undergo a supernova event, this clumping may ultimately lead to the formation of orbital bodies if the clumps acquire angular momentum with respect to the star via collisions with other clumps or other mechanisms.

[*]mwadas@umich.edu

[1] W. D. Arnett, J. N. Bahcall, R. P. Krishner, and S. E. Woosley, Supernova 1987A, Annu. Rev. Astron. Astrophys. **27**, 629 (1989).

[2] R. McCray, Supernova 1987A revisited, Annu. Rev. Astron. Astrophys. **31**, 175 (1993).

[3] R. McCray and C. Fransson, The remnant of Supernova 1987A, Annu. Rev. Astron. Astrophys. **54**, 19 (2016).

[4] B. E. K. Sugerman, A. P. S. Crotts, W. E. Kunkel, S. R. Heathcote, and S. S. Lawrence, The three-dimensional circumstellar environment of SN 1987A, Astrophys. J. Suppl. Ser. **159**, 60 (2005).

[5] C. Fransson, J. Larsson, K. Migotto, D. Pesce, P. Challis, R. A. Chevalier et al., The destruction of the circumstellar ring of SN 1987A, Astrophys. J. Lett. **806**, L19 (2015).

[6] NASA, ESA, CSA, M. Matsuura (Cardiff University), R. Arendt (NASA's Goddard Spaceflight Center & University of Maryland, Baltimore County), C. Fransson, https://www.nasa.gov/missions/webb/webb-reveals-new-structures-within-iconic-supernova/.

[7] N. Panagia, R. Gilmozzi, F. Macchetto, H.-M. Adorf, and R. P. Krishner, Properties of the SN 1987A circumstellar ring and the distance to the Large Magellanic Cloud, Astrophys. J. **380**, L23 (1991).

[8] B. A. Remington, J. Kane, R. P. Drake, S. G. Glendinning, K. Estabrook, R. London et al., Supernova hydrodynamics experiments on the Nova laser, Phys. Plasmas **4**, 5 (1997).

[9] E. Michael, R. McCray, C. S. J. Pun, P. Garnavich, P. Challis, R. P. Krishner et al., Hubble Space Telescope spectroscopy of spot 1 on the circumstellar ring of SN 1987A, Astrophys. J. **542**, L53 (2000).

[10] B. E. Sugerman, S. S. Lawrence, A. P. S. Crotts, P. Bouchet, and S. R. Heathcote, Evolution and geometry of hot spots in supernova remnant 1987A, Astrophys. J. **572**, 209 (2002).

[11] J. Larsson, C. Fransson, P. Gröningsson, A. Jerkstrand, C. Kozma, J. Sollerman et al., X-ray illumination of the ejecta of supernova 1987A, Nature (London) **474**, 23 (2011).

[12] T. T. Lim and T. B. Nickels, Instability and reconnection in the head-on collision of two vortex rings, Nature (London) **357**, 683 (1992).

[13] A. Crotts and S. Heathcote, Velocity structure of the ring nebula around supernova 1987A, Nature (London) **350**, 683 (1991).

[14] C. J. Burrows, J. Krist, J. J. Hester, R. Sahai, J. T. Trauger, K. R. Stapelfeldt et al., Hubble Space Telescope observations of the SN 1987A triple ring nebula, Astrophys. J. **452**, 680 (1995).

[15] N. Soker, Binary progenitor models for bipolar planetary nebulae, Astrophys. J. **496**, 833 (1998).

[16] T. Morris and P. Podsiadlowski, The triple-ring nebula around SN 1987A: Fingerprint of a binary merger, Science **315**, 1103 (2007).

[17] T. Morris and P. Podsiadlowski, A binary merger model for the formation of the supernova 1987A triple-ring nebula, Mon. Not. R. Astron. Soc. **399**, 515 (2009).

[18] L. Wang and P. A. Mazzali, Dynamical development of a ring-like structure in the supernova 1987A nebula, Nature (London) **355**, 58 (1992).

[19] S. M. Chiţă, N. Langer, A. J. van Marle, G. García-Segura, and A. Heger, Multiple ring nebulae around blue supergiants, Astron. Astrophys. **488**, L37 (2008).

[20] J. M. Blondin and P. Lundqvist, Formation of the circumstellar shell around SN 1987A, Astrophys. J. **405**, 337 (1993).

[21] T. Tanaka and H. Washimi, Formation of the three-ring structure around Supernova 1987A, Science **296**, 321 (2002).

[22] M. Akashi, E. Sabach, O. Yogev, and N. Soker, Forming equatorial rings around dying stars, Mon. Not. R. Astron. Soc. **453**, 2115 (2015).

[23] R. McCray and D. N. C. Lin, Is the ring around SN1987A a protostellar disk?, Nature (London) **369**, 378 (1994).

[24] P. Jakobsen, R. Albrecht, C. Barbieri, J. C. Blades, A. Boksenberg, P. Crane et al., First results from the faint object camera: SN 1987A, Astrophys. J. **369**, L63 (1991).

[25] G. Sonneborn, C. S. J. Pun, R. A. Kimble, T. R. Gull, P. Lundqvist, R. McCray et al., Spatially resolved STIS spectroscopy of SN 1987A: Evidence for shock interaction with circumstellar gas, Astrophys. J. **492**, L139 (1997).

[26] S. S. Lawrence, B. E. Sugerman, P. Bouchet, A. P. S. Crotts, R. Uglesich, and S. Heathcote, On the emergence and discovery of hot spots in SNR 1987A, Astrophys. J. **537**, L123 (2000).

[27] S. Park, S. A. Zhekov, D. N. Burrows, G. P. Garmire, and R. McCray, A Chandra view of the morphological and spectral evolution of supernova remnant 1987A, Astrophys. J. **610**, 275 (2004).

[28] S. Park, S. A. Zhekov, D. N. Burrows, J. L. Racusin, D. Dewey, and R. McCray, A new evolutionary phase of supernova remnant 1987A, Astrophys. J. Lett. **733**, L35 (2011).

[29] K. A. Frank, S. A. Zhekov, S. Park, R. McCray, E. Dwek, and D. N. Burrows, Chandra observes the end of an era in SN 1987A, Astrophys. J. **829**, 40 (2016).

[30] A. P. Ravi, S. Park, S. A. Zhekov, M. Miceli, S. Orlando, K. A. Frank, and D. N. Burrows, Spectral evolution of the x-ray remnant of SN 1987A: A high-resolution Chandra HETG study, Astrophys. J. **922**, 140 (2021).

[31] Y. Cendes, B. M. Gaensler, C.-Y. Ng, G. Zanardo, L. Staveley-Smith, and A. K. Tzioumis, The reacceleration of the shock wave in the radio remnant of SN 1987A, Astrophys. J. **867**, 65 (2018).

[32] J. Larsson, C. Fransson, D. Alp, P. Challis, R. A. Chevalier, K. Frank *et al.*, The matter beyond the ring: the recent evolution of SN 1987A observed by the Hubble Space Telescope, Astrophys. J. **886**, 147 (2019).

[33] S. Orlando, M. Miceli, M. L. Pumo, and F. Bocchino, Supernova 1987A: A template to link supernovae to their remnants, Astrophys. J. **810**, 168 (2015).

[34] Y. Zhou, Rayleigh-Taylor and Richtmyer-Meshkov instability induced flow, turbulence, and mixing. I, Phys. Rep. **720–722**, 1 (2017).

[35] Y. Zhou, Rayleigh-Taylor and Richtmyer-Meshkov instability induced flow, turbulence, and mixing. II, Phys. Rep. **723–725**, 1 (2017).

[36] Y.-G. Kang, H. Nishimura, H. Takabe, K. Nishihara, A. Sunhara, T. Norimatsu, K. Nagai, H. Kim, M. Nakatsuka, and H. J. Kong, Laboratory simulation of the collision of supernova 1987A with its circumstellar ring nebula, Plasma Phys. Rep. **27**, 843 (2001).

[37] S. Zhang, N. J. Zabusky, and K. Nishihara, Vortex structures and turbulence emerging in a supernova 1987A configuration: Interactions of "complex" blast waves and cylindrical/spherical bubbles, Laser Part. Beams **21**, 471 (2003).

[38] S. C. Crow, Stability theory for a pair of trailing vortices, AIAA J. **8**, 2172 (1970).

[39] T. Leweke and C. H. K. Williamson, Experiments on long-wavelength instability and reconnection of a vortex pair, Phys. Fluids **23**, 024101 (2011).

[40] T. Leweke, S. Le Dizès, and C. H. K. Williamson, Dynamics and instabilities of vortex pairs, Annu. Rev. Fluid Mech. **48**, 507 (2016).

[41] P. R. Spalart, Airplane trailing vortices, Annu. Rev. Fluid Mech. **30**, 107 (1998).

[42] C.-C. Chu, C.-T. Wang, C.-C. Chang, R.-Y. Chang, and W.-T. Chang, Head-on collision of two coaxial vortex rings: Experiment and computation, J. Fluid Mech. **296**, 39 (1995).

[43] R. McKeown, R. Ostilla-Mónico, A. Pumir, M. P. Brenner, and S. M. Rubinstein, Cascade leading to the emergence of small structures in vortex ring collisions, Phys. Rev. Fluids **3**, 124702 (2018).

[44] R. McKeown, R. Ostilla-Mónico, A. Pumir, M. P. Brenner, and S. M. Rubinstein, Turbulence generation through an iterative cascade of the elliptic instability, Sci. Adv. **6**, eaaz2717 (2020).

[45] Y. Qi, S. Tan, N. Corbitt, C. Urbanik, A. K. R. Salibindla, and R. Ni, Fragmentation in turbulence by small eddies, Nat. Commun. **13**, 1 (2022).

[46] W. T. Ashurst and D. I. Meiron, Numerical study of vortex reconnection, Phys. Rev. Lett. **58**, 1632 (1987).

[47] S. Kida and M. Takaoka, Vortex reconnection, Annu. Rev. Fluid Mech. **26**, 169 (1994).

[48] P. Chatelain, D. Kivotides, and A. Leonard, Reconnection of colliding vortex rings, Phys. Rev. Lett. **90**, 054501 (2003).

[49] J. Yao and F. Hussain, Vortex reconnection and turbulence cascade, Annu. Rev. Fluid Mech. **54**, 317 (2022).

[50] C. L. Martin and D. Arnett, The origin of the rings around SN1987A: An evaluation of the interacting-winds model, Astrophys. J. **447**, 378 (1995).

[51] T. Suzuki, T. Shigeyama, and K. Nomoto, X-ray emission from the collision of the ejecta with the ring nebula around SN 1987A, Astron. Astrophys. **274**, 883 (1993).

[52] M. Gharib, E. Rambod, and K. Shariff, A universal time scale for vortex ring formation, J. Fluid Mech. **360**, 121 (1998).

[53] K. Mohseni and M. Gharib, A model for universal time scale of vortex ring formation, Phys. Fluids **10**, 2436 (1998).

[54] P. Lundqvist and C. Fransson, Circumstellar emission from SN 1987A, Astrophys. J. **380**, 575 (1991).

[55] S. I. Braginskii, Transport processes in a plasma, Rev. Plasma Phys. **1**, 205 (1965).

[56] D. Ryutov, R. P. Drake, J. Kane, E. Liang, B. A. Remington, and W. M. Wood-Vasey, Similarity criteria for the laboratory simulation of supernova hydrodynamics, Astrophys. J. **518**, 821 (1999).

[57] M. J. Wadas, S. Balakrishna, H. J. LeFevre, C. C. Kuranz, A. Towne, and E. Johnsen, On the stability of a pair of vortex rings, J. Fluid Mech. **979**, A3 (2024).

[58] J. Norbury, A family of steady vortex rings, J. Fluid Mech. **57**, 417 (1973).

[59] R. T. Pierrehumbert, A family of steady, translating vortex pairs with distributed velocity, J. Fluid Mech. **99**, 129 (1980).

[60] J. Jeong and F. Hussain, On the identification of a vortex, J. Fluid Mech. **285**, 69 (1995).

[61] J. J. Haas and B. Sturtevant, Interaction of weak shock waves with cylindrical and spherical gas inhomogeneities, J. Fluid Mech. **181**, 41 (1987).

[62] D. Olmstead, P. Wayne, J. H. Yoo, S. Kumar, C. R. Truman, and P. Vorobieff, Experimental study of shock-accelerated inclined heavy gas cylinder, Exp. Fluids **58**, 71 (2017).

[63] W. Zhang, A. Almgren, V. Beckner, J. Bell, J. Blaschke, C. Chan *et al.*, AMReX: A framework for block-structured adaptive mesh refinement, J. Open Source Softwaare **4**, 37 (2019).

[64] J. C. R. Hunt, A. A. Wray, and P. Moin, Eddies, streams, and convergence zones in turbulent flows, Center for Turbulence Research Report CTR-S88 (1988), https://ntrs.nasa.gov/citations/19890015184.

[65] S. Mattila, P. Lundqvist, P. Gröningsson, P. Meikle, R. Stathakis, C. Fransson, and R. Cannon, Abundances and density structure of the inner circumstellar ring around SN 1987A, Astrophys. J. **717**, 1140 (2010).

[66] S. A. Zhekov, S. Park, R. McCray, J. L. Racusin, and D. N. Burrows, Evolution of the Chandra CCD spectra of SNR 1987A: Probing the reflected-shock picture, Mon. Not. R. Astron. Soc. **407**, 1157 (2010).

[67] D. Dewey, V. V. Dwarkadas, F. Haberl, R. Strum, and C. R. Canizares, Evolution and hydrodynamics of the very broad

x-ray line emission in SN 1987A, Astrophys. J. **752,** 103 (2012).

[68] S. Orlando, M. Ono, S. Nagataki, M. Miceli, H. Umeda, G. Ferrand *et al.*, Hydrodynamic simulations unravel the progenitor-supernova-remnant connection in SN 1987A, Astron. Astrophys. **636,** A22 (2020).

[69] R. A. Chevalier and V. V. Dwarkadas, The presupernova H II region around SN 1987A, Astrophys. J. Lett. **452,** L45 (1995).

[70] M. J. Wadas, L. H. Khieu, G. S. Cearley, H. J. LeFevre, C. C. Kuranz, and E. Johnsen, Saturation of vortex rings ejected from shock-accelerated interfaces, Phys. Rev. Lett. **130,** 194001 (2023).

[71] F. Bertoldi, The photoevaporation of interstellar clouds. I. Radiation-driven implosion, Astrophys. J. **346,** 735 (1989).

[72] N. Smith and R. McCray, High resolution spectroscopy of SN1987A's rings: He I λ10830 and $H\alpha$ from the hotspots, AIP Conf. Proc. **937,** 179 (2007).

[73] A. C. Boley, M. J. Payne, S. Corder, W. R. F. Dent, E. B. Ford, and M. Shabram, Constraining the planetary system of Fomalhaut using high-resolution ALMA observations, Astrophys. J. Lett. **750,** L21 (2012).

[74] H. E. Bond, D. L. Pollacco, and R. F. Webbink, WeBo 1: Young barium star surrounded by a ringlike planetary nebula, Astron. J. **125,** 260 (2003).

[75] N. Smith, W. D. Arnett, J. Bally, A. Ginsburg, and A. V. Filippenko, The ring nebula around the blue supergiant SBW1: Pre-explosion snapshot of an SN 1987A twin, Mon. Not. R. Astron. Soc. **429,** 1324 (2013).

[76] G. M. Kennedy, S. Marino, L. Matrà, O. Panić, D. Wilner, M. C. Wyatt, and B. Yelverton, ALMA observations of the narrow HR 4796A debris ring, Mon. Not. R. Astron. Soc. **475,** 4924 (2018).

[77] G. M. Kennedy, L. Matrà, S. Facchini, J. Milli, O. Panić, D. price, D. J. Wilner, M. C. Wyatt, and B. Yelverton, A circumbinary protoplanetary disk in a polar configuration, Nat. Astron. **3,** 230 (2019).

[78] S. M. Andrews, J. Huang, L. M. Pérez, A. Isella, C. P. Dullemond, N. T. Kurtovic *et al.*, The disk substructures at high angular resolution project (DSHARP). I. Motivation, sample, calibration, and overview, Astrophys. J. Lett. **869,** L41 (2018).